THE JOURNAL OF BIOLOGICAL CHEMISTRY VOL. 281, NO. 31, pp. 21799–21812, August 4, 2006

Mathematical Modeling of Polyamine Metabolism in Mammals*[S]

Received for publication, March 23, 2006, and in revised form, May 17, 2006 Published, JBC Papers in Press, May 18, 2006, DOI 10.1074/jbc.M602756200

Carlos Rodríguez-Caso[‡1], **Raúl Montañez**[‡], **Marta Cascante**[§], **Francisca Sánchez-Jiménez**[‡], **and Miguel A. Medina**[‡2]

From the [‡]*Departamento de Biología Molecular y Bioquímica, Facultad de Ciencias, Universidad de Málaga, Málaga E-29071, Spain and* [§]*Departamento de Bioquímica, Facultad de Química, Universidad de Barcelona, Barcelona E-08028, Spain*

Polyamines are considered as essential compounds in living cells, since they are involved in cell proliferation, transcription, and translation processes. Furthermore, polyamine homeostasis is necessary to cell survival, and its deregulation is involved in relevant processes, such as cancer and neurodegenerative disorders. Great efforts have been made to elucidate the nature of polyamine homeostasis, giving rise to relevant information concerning the behavior of the different components of polyamine metabolism, and a great amount of information has been generated. However, a complex regulation at transcriptional, translational, and metabolic levels as well as the strong relationship between polyamines and essential cell processes make it difficult to discriminate the role of polyamine regulation itself from the whole cell response when an experimental approach is given *in vivo*. To overcome this limitation, a bottom-up approach to model mathematically metabolic pathways could allow us to elucidate the systemic behavior from individual kinetic and molecular properties. In this paper, we propose a mathematical model of polyamine metabolism from kinetic constants and both metabolite and enzyme levels extracted from bibliographic sources. This model captures the tendencies observed in transgenic mice for the so-called key enzymes of polyamine metabolism, ornithine decarboxylase, *S*-adenosylmethionine decarboxylase and spermine spermidine *N*-acetyl transferase. Furthermore, the model shows a relevant role of *S*-adenosylmethionine and acetyl-CoA availability in polyamine homeostasis, which are not usually considered in systemic experimental studies.

During much of the last century, biology was an attempt to reduce biological phenomena to the behavior of molecules. Despite the enormous success of this approach, most biological functions arise from interactions among many components, yielding nonlinear behavior that has been fine tuned by natural selection to achieve specific functional properties (1, 2). Therefore, a comprehensive understanding of biological functions requires a new systemic perspective. In the last few years, systems biology and synthetic biology have emerged to fulfill this goal (3–5). Systems biology approaches are hypothesis-driven and involve iterative rounds of model building, prediction, experimentation, and model refinement and development (6, 7). Computer science development is allowing faster and faster numerical simulations of mathematical models. Interesting and relevant mathematical models of several well known metabolic pathways have been published very recently (8–10). Far from replacing knowledge acquisition from experimental evidence, mathematical modeling allows to test and define more accurately hypothesis that have to be experimentally tested later. Furthermore, modeling allows to build a comprehensive framework based on a compilation of the experimental data provided by the scientific community. With this philosophy, we propose and study a mathematical model of polyamine metabolism. We will see that polyamine metabolism exhibits some features that, on one hand, make possible the modeling task and, on the other, make modeling an excellent tool to propose novel hypotheses to be tested.

Ornithine-derived polyamines (putrescine, spermidine, and spermine) are biogenic low molecular weight organic polycations that are present in all living organisms. They have pleiotropic effects, with a recognized major role as metabolic regulators of the rate and fidelity of macromolecular synthesis, cell proliferation/death balance, and cell differentiation, among others (11–15). Direct interactions between polyamines and nucleic acids (16, 17), proteins (18–21), and biological membranes (22) have been proposed to explain some of these biological functions. In fact, estimations of noncovalent polyamine binding to macromolecules suggest that only around 10% of total polyamines are free in mammalian cells (23, 24). Furthermore, it is noteworthy that polyamines are involved in the regulation of the expression of certain genes by means of polyamine response elements in their promoters (25, 26). Intracellular levels of polyamines must be maintained within narrow limits, since a decrease of polyamine levels interferes with cell growth, whereas an excess appears to be toxic (27–29). In fact, a deregulation of polyamine metabolism is related to different pathologies, such as cancer (16), psoriasis (30), and neurodegenerative diseases (19, 20). Polyamine-cancer connections have been extensively studied for decades, pointing to inhibition of polyamine synthesis or activation of polyamine catabolism as a potential cancer chemopreventive strategy (31–33). Polyamine metabolism in cancer is a good example of a process showing a strong interweaving between interacting genes and metabolites, since specific oncogenes and tumor suppressor are

* This work was supported by Andalusian Government Grants SAF2005-01812 and funds to group CVI-267 and to the "Amine System Project" (CVI-657) (to M. A. M. and F. S.-J.) and Ministerio de Ciencia y Tecnología, Spain, Grant SAF2005-01627 (to M. C.). The costs of publication of this article were defrayed in part by the payment of page charges. This article must therefore be hereby marked "*advertisement*" in accordance with 18 U.S.C. Section 1734 solely to indicate this fact.

[S] The on-line version of this article (available at http://www.jbc.org) contains Equations 1–18 and Tables S1 and S2.

[1] Recipient of a fellowship from the Spanish Ministry of Education and Science. Present address: Complex Systems Lab, Universitat Pompeu Fabra, Dr. Aiguader 80, Barcelona 08003, Spain.

[2] To whom correspondence should be addressed. Tel.: 34-95-2137132; Fax: 34-95-2132000; E-mail: medina@uma.es.

regulators of polyamine metabolism, and polyamine levels affect the rate of cell proliferation (34–37).

Due to the pleiotropic and important roles of polyamines, their metabolism has long been the focus of biochemical studies that have provided extensive and detailed information concerning each of the enzymes and metabolites of the pathway (22, 38, 39). However, most of this information is very disperse and not integrated in a comprehensive, systemic framework. On the other hand, many therapeutic strategies based on the specific inhibition of one of the key enzymes of polyamine metabolism have failed, mostly due to the presence of compensating mechanisms in polyamine metabolism that contribute to the buffering of those effects elicited when only an enzyme is the target (15, 40). The structure of the reaction diagram of polyamine metabolism in mammals is relatively complex, consisting of a bi-cycle having two required entrances (ornithine and *S*-adenosylmethionine) and several alternative exits (Fig. 1). For most of the reactions, both activities and turnover rates of enzymes depend on polyamine concentrations in a nonlinear way. Therefore, the behavior of the full pathway in response to genetic and environmental perturbations cannot be easily deduced from the reaction diagram itself. Nevertheless, if the behavior of the elements of a system is known, they can be assembled in a model to acquire a global knowledge of the system. This is known as a bottom-up approach. In this case, the global behavior of polyamine metabolism taken as a biomodule (1) can be investigated with a mathematical model, which describes the reactions and interactions among its components. This will allow us to ascertain whether potential strong modulators of polyamine metabolism are expected to induce relevant effects administered either alone or in combination.

In this paper, the first basic mathematical modeling of polyamine metabolism in mammals is described. It is based on available experimental metabolite concentrations and kinetic data. This work is carried out under the philosophy of a modeling-testing recursive operation, in order to obtain the minimal model able to capture the majority of tendencies observed in the literature. By means of this process, starting from the model shown in Fig. 1*A* (which includes the enzymes and metabolites usually determined in experimental studies concerning polyamine metabolism), we obtained a model that considers the study system shown in Fig. 1*B*, which includes *S*-adenosylmethionine (SAM)[3] as a variable and takes into account acetyl-CoA availability. Our model does not, at this stage, include details, such as polyamine and cationic amino acid transport, compartmentalization, and detailed gene expression regulation (22, 41). Despite these simplifications, this basic model reproduces and explains many experimental findings. Furthermore, this modeling contributes to and aims at understanding the emergent properties of this nonlinear complex-interconnected biomodule and its responses to genetic and environmental variations.

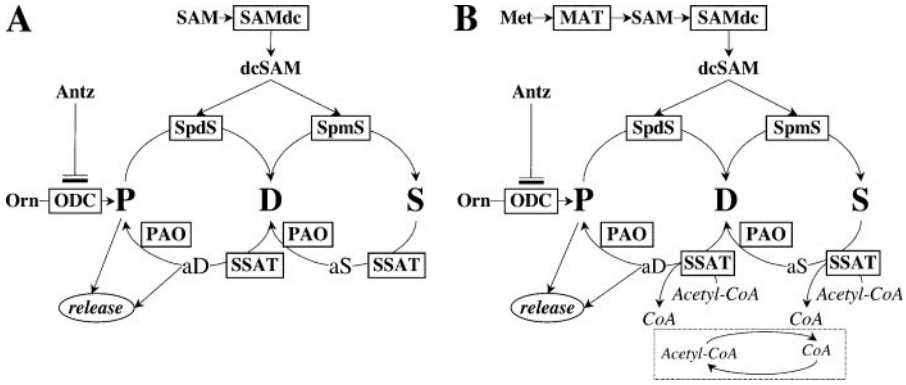

FIGURE 1. **Polyamine metabolism.** Components considered in the initial (*A*) and further versions (*B*) of the model are shown. The acetyl-CoA/CoA recycling, only considered in the final version of the model, is represented as a *dotted box*.

MATERIALS AND METHODS

Study System Definition and Mathematical Model Description—We built a mathematical model of mammalian polyamine metabolism (Fig. 1) from metabolite concentrations and enzymic constants (Michaelis constants, inhibitory constants, and activities) derived from relevant published studies carried out by expert groups actively involved in polyamine research. The limits of the system under study were defined by an iterative process of model refinement in order to achieve the simplest model able to capture the more relevant features of polyamine metabolism. We started with a basic model, where we only considered the bi-cyclic central core for the interconversion of putrescine, spermidine, and spermine, with ornithine and SAM as entries of the system (Fig. 1*A*). The initial versions of the model consider the enzyme activities and polyamine concentrations usually taken into account and determined in experimental studies. As a result of this iterative modeling process, we propose in this paper an extended version of this study system (Fig. 1*B*), where entries are through ornithine decarboxylase (ODC) and methionine adenosyltransferase. Their respective substrates, ornithine and methionine, were considered parameters in our model. We also took into account the role of acetyl-CoA as a cosubstrate in polyamine acetylation reactions.

The study system proposed in Fig. 1*B* was modeled by taking into account some assumptions. The entries of the model (ornithine, methionine, and acetyl-CoA) were considered as parameters. Putrescine and acetylspermidine were the unique molecular species able to go out of the model. This simplification was done based on studies with cultured cells showing that, indeed, putrescine and acetylspermidine are the major forms of polyamine release (42). These releases were modeled by simple, linear equations. Terminal catabolism of putrescine by diamine

[3] The abbreviations used are: SAM, *S*-adenosylmethionine; SSAT, spermidine/spermine acetyltransferase; P, putrescine; D, spermidine; S, spermine; A, decarboxylated *S*-adenosylmethionine; aD, *N*-acetylspermidine; aS, *N*-acetyl-spermine; Antz, antizyme; MAT, methionine adenosyltransferase; ODC, ornithine decarboxylase; SAMdc, S-adenosylmethionine decarboxylase; SpdS, spermidine synthase; SpmS, spermine synthase; PAO, polyamine oxidase; 5′MTA, 5′-methylthioadenosine; DFMO, difluoromethylornithine; MGBG, methylglyoxalbis(guanylhidrazone).

TABLE 1
Rate equations for enzymes and processes included in the model

Equations and parameters	Description
ODC $v_{ODC} = \frac{V_{\max}^{ODC} \cdot [Orn]}{K_M^{ODC}\left(1+\frac{[P]}{K_{ip}^{ODC}}\right)+[Orn]}$	Michaelis-Menten equation with competitive inhibition by putrescine. Level of ODC activity is a time-dependent variable according to a modified Schimke equation, where polyamines affect to synthesis rate
SAMdc $v_{SAMdc} = \frac{V_{\max}^{SAMdc}}{1+\frac{[S]}{K_{is}^{SAMdc}}} \cdot \frac{[SAM]}{K_M^{SAMdc}\left(1+\frac{K_{aP}^{SAMdc}}{P}+\frac{[A]}{K_{iA}^{SAMdc}}\right)+[SAM]}$	Michaelis behavior with non-competitive inhibition by spermine, activation by putrescine and competitive inhibition by decarboxylated SAM (96). Activity is a time-dependent variable described by modified Schimke equation where synthesis rate is modulated negatively by polyamines.
SSAT for D $v_{SSATD} = \frac{V_{\max}^{SSAT} \cdot [D] \cdot [acCoA]}{K_{MD}^{SSAT}\left(1+\frac{[S]}{K_{MS}^{SSAT}}\right) \cdot K_{MacCoA}^{SSAT}\left(1+\frac{[CoA]}{K_{MCoA}^{SSAT}}\right)+K_{MacCoA}^{SSAT}\left(1+\frac{[CoA]}{K_{MCoA}^{SSAT}}\right)[D]+K_{MD}^{SSAT}\left(1+\frac{[S]}{K_{MS}^{SSAT}}\right)[acCoA]+[D] \cdot [acCoA]}$ **SSAT for S** $v_{SSATS} = \frac{1}{C} \frac{V_{\max}^{SSAT} \cdot [S] \cdot [acCoA]}{K_{MS}^{SSAT}\left(1+\frac{[D]}{K_{MD}^{SSAT}}\right) \cdot K_{MacCoA}^{SSAT}\left(1+\frac{[CoA]}{K_{MCoA}^{SSAT}}\right)+K_{MacCoA}^{SSAT}\left(1+\frac{[CoA]}{K_{MCoA}^{SSAT}}\right)[S]+K_{MS}^{SSAT}\left(1+\frac{[D]}{K_{MD}^{SSAT}}\right)[acCoA]+[S] \cdot [acCoA]}$	Michaelis equations for enzymes able to catalyze more than one reaction. Activity is a time-dependent variable defined by modified Schimke equation. Polyamines activate synthesis and inhibit degradation. C is a correction factor according to the observation that SSAT catalyzes spermidine acetylation 4.44 times faster than spermine acetylation (97).
PAO for aD $v_{PAOaD} = \frac{V_{\max}^{PAO} \cdot [aD]}{K_{MaD}^{PAO}\left(1+\frac{[aD]}{K_{MaD}^{PAO}}+\frac{[aS]}{K_{MaS}^{PAO}}+\frac{[D]}{K_{MD}^{PAO}}+\frac{[S]}{K_{MS}^{PAO}}\right)}$ **PAO for aS** $v_{PAOaS} = \frac{V_{\max}^{PAO} \cdot [aS]}{K_{MaS}^{PAO}\left(1+\frac{[aD]}{K_{MaD}^{PAO}}+\frac{[aS]}{K_{MaS}^{PAO}}+\frac{[D]}{K_{MD}^{PAO}}+\frac{[S]}{K_{MS}^{PAO}}\right)}$	Michaelis equations for enzymes able to catalyze more than one reaction with competitive inhibition by spermine and spermidine. Inhibitor constants for those polyamines are the respective Michaelis constants. However, the direct metabolization of polyamines by PAO is not allowed in this model.
SpdS $v_{SpdS} = \frac{V_{\max}^{SpdS} \cdot [A][P]}{K_{ia}^{SpdS} \cdot K_P^{SpdS}\left(1+\frac{[D]}{K_{iD}^{SpdS}}\right)+K_P^{SpdS}[A]+K_A^{SpdS}\left(1+\frac{[D]}{K_{iD}^{SpdS}}\right)[P]+[A][P]}$	Equation was taken from (47) and it was simplified (5'MTA was not taken into account).
SpmS $v_{SpmS} = \frac{V_{\max}^{SpmS} \cdot [A][D]}{K_{ia}^{SpmS} \cdot K_D^{SpmS}\left(1+\frac{[S]}{K_{iS}^{SpmS}}\right)+K_D^{SpmS}[A]+K_A^{SpmS}\left(1+\frac{[S]}{K_{iS}^{SpmS}}\right)[D]+[A][D]}$	Equation was taken from (48) and it was simplified (5'MTA was not taken into account).
MAT $v_{MAT} = \frac{V_{\max}^{MAT}}{1+\left(\frac{K_M^{MAT}}{[Met]}\right) \cdot \left(1+\left(\frac{[SAM]}{K_{iMet}^{MAT}}\right)\right)}$	Kinetic equation taken from (8,98) for MAT isoenzyme I. SAM has an inhibitory effect.
Acetyl-CoA/CoA recycling $v_{acCoA} = k_{acCoA} \cdot [CoA]$ $v_{CoA} = k_{CoA} \cdot [acCoA]$	Cycle of synthesis and degradation of acetyl-CoA by different metabolic reactions.
P efflux $v_{Pefflux} = k_P^{efflux} \cdot [P]$	Linear equation with tuned parameter
aD efflux $v_{aDefflux} = k_{aD}^{efflux} \cdot [aD]$	Linear equation with tuned parameter

TABLE 2

Differential equations for the different metabolites and other time-dependent variables included in the model

Metabolite-dependent velocities are indicated by combining both enzyme and metabolite abbreviations as the subscripted notations. (*e.g.* V_{SSATD}, SSAT velocity for spermidine; V_{PAOaS}, PAO velocity for acetylated spermine, etc.) AcCoA, acetyl-CoA.

Time-dependent variables	Differential equations
$[P]$	$\frac{d[P]}{dt} = v_{ODC} + v_{PAOaS} - v_{SpdS} - v_{Pefflux}$
$[D]$	$\frac{d[D]}{dt} = v_{SpdS} + v_{PAOaS} - v_{SpmS} - v_{SSATD}$
$[S]$	$\frac{d[S]}{dt} = v_{SpmS} - v_{SSATS}$
$[SAM]$	$\frac{d[SAM]}{dt} = v_{MAT} - v_{SAM}$
$[A]$	$\frac{d[A]}{dt} = v_{SAMdc} - v_{SpdS} - v_{SpmS}$
$[aD]$	$\frac{d[aD]}{dt} = v_{SSATD} - v_{PAOaD} - v_{aDefflux}$
$[aS]$	$\frac{d[aS]}{dt} = v_{SSATS} - v_{PAOaS}$
$[acCoA]$	$\frac{d[acCoA]}{dt} = v_{acCoA} - v_{CoA} - v_{SSATS} - v_{SSATD}$
$[CoA]$	$\frac{d[CoA]}{dt} = v_{CoA} + v_{SSATS} + v_{SSATD} - v_{acCoA}$
$V_{\max}^{ODC}$	$\frac{dV_{\max}^{ODC}}{dt} = k_s^{ODC}\left(\frac{1}{1+\left(K_{eq}^{ODC}([D]+[S])\right)}\right) - k_d^{ODC}\cdot Antz\cdot V_{\max}^{ODC}$
$Antz$	$\frac{dAntz}{dt} = k_s^{Antz}\left(1-\frac{1}{1+K_{eq}^{Antz}([D]+[S])}\right) - k_d^{Antz}\cdot Antz$
$V_{\max}^{SAMdc}$	$\frac{dV_{\max}^{SAMdc}}{dt} = k_s^{SAMdc}\left(\frac{1}{1+\left(K_{eq}^{SAMdc}([D]+[S])\right)}\right) - k_d^{SAMdc}\cdot V_{\max}^{SAMdc}$
$V_{\max}^{SSAT}$	$\frac{dV_{\max}^{SSAT}}{dt} = k'^{SSAT}_s\left(1-\frac{1}{1+\left(K_{eq}^{SSAT}([D]+[S])\right)}\right) - k_d^{SSAT}\left(\frac{1}{1+\left(K_{eq}^{SSAT}([D]+[S])\right)}\right)V_{\max}^{SSAT}$

oxidase was not included in the model, since this activity is unevenly distributed in mammals and terminal catabolism appears to be restricted to selected tissues (43, 44). In any case, due to the nature of the "efflux" in our model, putrescine release can also be considered as a combination of putrescine "efflux" plus terminal catabolism for this diamine. Antizyme, a small regulatory protein regulated by polyamine levels (45) with a key role in ODC degradation (28, 39, 46), was included in the model. SAM availability was taken into account by introducing in the model the rate equation assumed in a methionine cycle model published recently (8). For acetyl-CoA availability, we assumed a linear interconversion between acetyl-CoA and CoA, taking the acetyl-CoA + CoA pool and the recycling rate *R* as parameters. This assumption is based on the postulate that, under certain conditions, SSAT inductions can deplete acetyl-CoA levels. Other aspects, such as polyamine and cationic amino acid transport, compartmentalization, and detailed gene expression regulatory features (22, 41), were not included in the model at the present stage.

Table 1 gives the rate equations for all of the enzymes included in the model, along with a brief description of their features. For the bisubstrate enzymes spermidine and spermine synthases (SpdS and SpmS), the inhibitory effect of the subproduct 5′-methylthioadenosine (5′MTA) was omitted. We assumed in the model that 5′MTA was virtually zero. This assumption was supported by the fact that 5′MTA is quickly removed by 5′MTA phosphorylase (47, 48). Table 2 gives the differential equations for the different metabolites and other time-dependent variables. More details on relevant features of the enzymes included in the model are given in the supplemental materials.

Model Implementation and Initial Conditions—The model was implemented in Perl language (available on the World

TABLE 3

Comparison of the predictive capabilities of the different versions of the model

In all cases, overexpressions were simulated by increasing 100 times the basal level of the respective activity.

Description	ODC overexpression	SSAT overexpression	SAMdc overexpression
Version 1 Components are shown in Fig. 1*A*. Activities are considered as parameters.	Polyamine homeostasis and high putrescine increases[a]	Polyamine depletion and putrescine homeostasis	Fast increases to nonphysiological levels of polyamines
Version 2 Components are shown in Fig. 1*B*. Activities, [acetyl-CoA] and [CoA], are considered as parameters.	Polyamine homeostasis and high putrescine increases[a]	Polyamine depletion and putrescine homeostasis	Slow responses tending to increase polyamine levels
Version 3 Components are shown in Fig. 1*A*. ODC, SAMdc, and SSAT activities are considered as time-dependent variables.	Polyamine homeostasis and high putrescine increases[a]	Polyamine depletion and increases of both ODC and putrescine[a]	Increases of polyamine levels
Version 4 (final model) Components are shown in Fig. 1*B*. ODC, SAMdc, and SSAT activities are considered as time-dependent variables. [Acetyl-CoA]/[CoA] recycling is considered.	Polyamine homeostasis and high putrescine increases[a]	Polyamine depletion or homeostasis (depending on the acetyl-CoA availability) and increases of both ODC and putrescine[a]	Polyamine homeostasis[a]

[a] Results according to the major tendencies reported in the literature.

TABLE 4

Polyamine concentrations and enzyme activities considered as the *basal conditions* in the final model compared with those calculated from data in Ref. 58

	Free polyamine concentrations			Enzyme activities			[Antz]
	Putrescine	Spermidine	Spermine	ODC	SSAT	SAMdc	
		μM			μM min^{-1}		μM
Data from Ref. 58	131.9	91.4	38.5	9.5	Not given	0.30	Not given
Data from the model	109.4	73.4	53.4	1.6	1.3	0.9	0.6

Wide Web at www.perl.com/). Perl is a multiplatform, free, and easy-to-learn programming language commonly used by bioinformaticians. Furthermore, the use of Perl allows the solution of complex differential equation systems with low computational cost, due to its simplicity and its capability to work without the requirement of a graphic interface. Nonetheless, other programming languages, such as Python, can also be used for implementation of the model. Whatever the programming language used, our program is a script of instructions with the following basic structure: 1) parameter definition; 2) definition of initial conditions for all of the variables; 3) beginning of an iterative loop ((*a*) calculation of velocities from differential equations providing the current values of variables; (*b*) updating of the variable values by multiplying velocities by step size; (*c*) calculation of the current simulation time by multiplying the number of iterations by the step size; (*d*) collection of variables and time in a file); 4) end of program.

Simulations were carried out by the iterative Euler method, with a time increment of 0.01 min/iteration. For numerical simulations of the model, a PC with an AMD-K7 Athlon 1800 XP microprocessor with Linux as the operating system and an Apple Macintosh Powerbook G4 with MacOS X were used interchangeably.

Table S1 shows the ranges of values available in literature for the parameters considered in our model as well as our initial choices for the simulations. For those parameters with no available reference in the literature, the values included in the model for simulations were chosen by initial "tuning," an optimization process to achieve steady states within the physiological range of values for the elements included in the system. Physiological levels of polyamines are found in cultured cells in the submillimolar range, and activities are in the range of μM min^{-1} (23, 49–54). In order to analyze the behavior of these "tuned" parameters in the acquisition of steady states, we carried out additional simulations, changing their values by a factor of 0.1 or 100.

On the other hand, since polyamines are distributed among free and noncovalently bound polyamine pools *in vivo*, we tuned the model to respond to free polyamines, taking the free polyamine/total polyamine ratio as a constant. As previously mentioned, ~10% of total polyamines (spermine and spermidine) are estimated to be free in living cells according to the literature (23, 24). In this work, [S] and [D] values (spermine and spermidine in mathematical model notation, respectively) are shown as free polyamine concentrations.

Since activities and polyamine levels available in the literature are expressed with respect to the total amount of protein or number of cells, we converted these units to μM min^{-1} (activities) and μM (metabolites). For these conversions, we took 2 pl as a mean cellular volume, as well as the equivalence of 100 μg of protein contained in 10^6 cells (55).

In all of the simulations, steady state was considered to be reached when the change of any variable was lower than 10^{-12} within an interval of 3 h (18,000 iterations).

Sensitivity Analysis—Sensitivity analysis determines the relative importance of the different parameters to induce

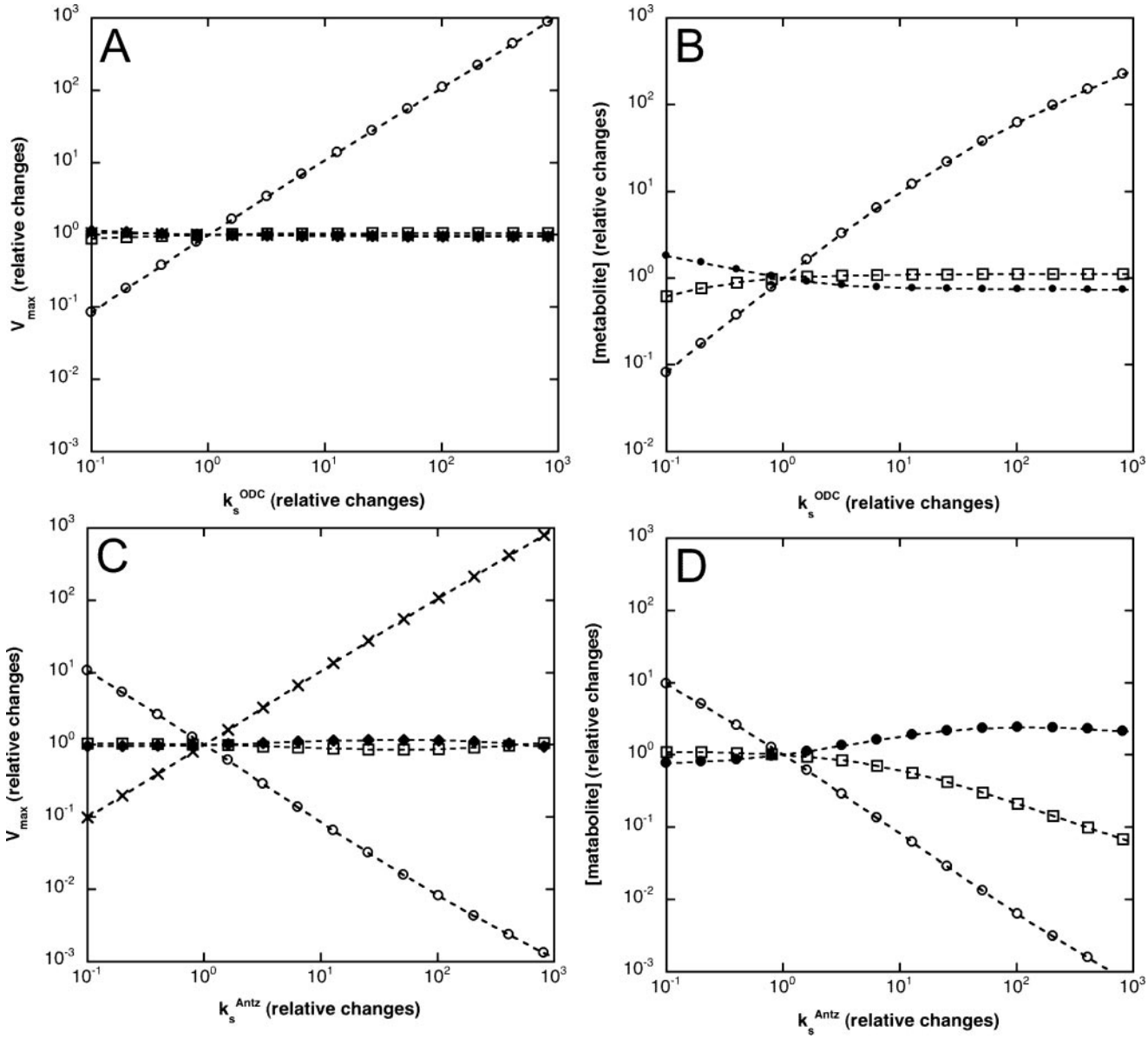

FIGURE 2. **Effects of changes in ODC k_S (*A* and *B*) and Antz k_S (*C* and *D*) on time-dependent activities (*A* and *C*) (ODC (*empty circles*), Antz (*crosses*), SSAT (*black diamonds*), and SAMdc (*empty squares*)) and on metabolite levels (*B* and *D*) (putrescine (*empty circles*), spermidine (*empty squares*), and spermine (*full circles*)), relative to the basal condition steady state.**

changes in time-dependent variables. From an initial steady state, an infinitesimal change in the value of a parameter is introduced, and the global changes in the system are evaluated after acquiring a new steady state. Detailed information on how this kind of analysis was carried out can be found in the supplemental material.

In Silico Simulations of Experiments Representing Gene or Environmental Changes—We focused our studies on inductions and inhibitions of the three enzymes described as rate-limiting of the overall metabolic pathway, namely, ODC, SAMdc, and SSAT (13). As detailed in the supplemental material, these three key enzymes and the regulator antizyme have turnover rates that depend on polyamine concentrations, a key feature taken into account in our model. To simulate gene manipulation leading to induction (overexpression), two different approaches were used. We tested the effects of different increases (1–1000-fold) in the values of the respective k_s parameters. In other cases, inductions were simulated by direct increase of the respective values of activities in the basal conditions, taking those activities not as time-dependent variables but, on the contrary, as time-independent parameters. Down-regulations of rate-limiting enzyme activities were simulated by up to 10-fold decreases of k_s values. We also simulated pharmacological interventions leading to inhibition of ODC and SAMdc by difluoromethylornithine (DFMO) and methylglyoxalbis(guanylhidrazone) (MGBG), respectively (22). For ODC inhibition with DFMO, its activity was treated as a time-independent parameter and received a value of zero, since DFMO is described as a irreversible inhibitor of ODC (56). However, concerning SAMdc inhibition, the competitive inhibitor MGBG (57) was considered to produce a potent decrease

(90%) of activity. To simulate ODC, SAMdc, and SSAT alterations caused by the polyamine analog DENSPM (N^1,N^{11}-diethylnorspermidine) at a 1 mM intracellular concentration (58), we considered it as a structural analog of higher polyamines; thus, we replaced ([D] + [S]) by ([D] + [S] + 1000) in the equations for the time-dependent enzymes described in Table 2. All of the time response effects were simulated for 96 h (576,000 iterations).

RESULTS AND DISCUSSION

From the Core System Model to Our Final Model: Iterative Model Refinement—A main goal of modeling is to discern the minimal relevant processes able to explain the majority of experimental data concerning the behavior of the modeled system. As mentioned above, we started with a core system model (Fig. 1*A*) based on those elements of polyamine metabolism usually taken into account in experimental studies. This core system was properly modeled defining the involved rate velocity equations, maintaining fixed all involved enzymic activities; later, it was extended to include differential equations of time-dependent variables and initial conditions. The procedure was similar to that described under "Materials and Methods" and shown in Tables 1, 2 and S1) for our final model (Fig. 1*B*). For the sake of simplicity, herein we only show details concerning the final model, but simulations of the core system model yielded a physiological basal steady state and sensitivity analysis showing that this model was robust (results not shown). Furthermore, this core system model was good enough to simulate properly much of the available experimental data concerning modulation (overexpression or inhibition) of three key enzymes (see Table 3), with the exception of some features of SAMdc and SSAT modulation that could not be well simulated (discussed below). However, this is not a limitation of modeling; on the contrary, this kind of disagreement regarding available experimental results is a sign of the predictive potential of the modeling approach, since it points out some essential aspects not usually taken into account in experimental studies of polyamine metabolism modulation. Concretely, simulations of the core system model described in Fig. 1*A* suggested that SAM and acetyl-CoA (two metabolites not included in the core system model) could play a main role in this metabolic pathway. To test this hypothesis, we carried out an iterative model refinement leading to the model shown in Fig. 1*B*. More details are given in the supplemental material. Table 3 summarizes the comparative predictive capabilities of the models generated and tested during this iterative refinement process. As stated above, from now on, we only present details concerning the model represented in Fig. 1*B*.

Initial Conditions, Steady State Acquisition, and Sensitivity Analysis of the Model—As shown in Table S1 of the supplemental materials and mentioned above, several parameters of the model were not directly available in the scientific literature. They include the equilibrium constants for the interaction of polyamines with the enzymes regulated by their concentrations (ODC, SAMdc, and SSAT), the velocity constants for synthesis and degradation in the modified Schimke equations, the inhibition constant for spermidine on spermine synthase activity, and the velocity constants in the linear equations for effluxes.

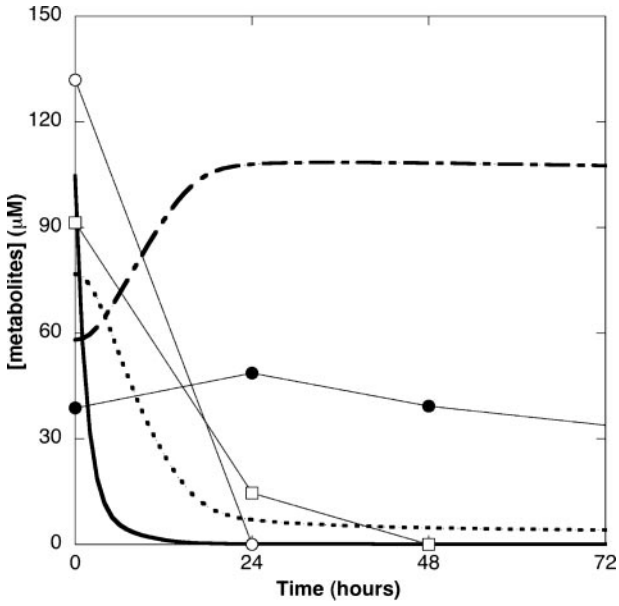

FIGURE 3. **DFMO effects on polyamine levels in both time-response simulations and data extracted from Ref. 58.** *In silico* experiments are shown as follows: putrescine (*continuous line*), spermidine (*dotted line*), and spermine (*segment and dotted line*). Experimental data are shown as follows: putrescine (*empty circles*), spermidine (*empty squares*), and spermine (*full circles*).

For these parameters, the model reached steady state over a wide range of initial values tested. However, as described under "Materials and Methods," the specific values finally included as initial conditions (Table S1) were selected by a "tuning" of the model in order to obtain physiological levels of polyamines and enzyme activities. A lack of experimental data frequently imposes such kinds of adjustments for the proper performance of mathematical models of metabolic pathways (9). Nonetheless, half-life values for the short lived enzymes ODC, SAMdc, and SSAT are available in the literature, and they can be used to check whether the k_D values selected by "tuning" of the model were out of range or not. From these values, theoretical half-lives of ODC, SAMdc, and SSAT are calculated to be 14, 9, and 10 min, respectively. These three values agree with those previously reported in experimental works. In fact, mammalian ODC is described as having a half-life of minutes, as short as 5 min (59); for SAMdc, half-life determined experimentally is around 20 min (59); and, finally, SSAT overexpressed in COS-7 cells has a half-life of 20 min (60).

Simulations of the model described in Fig. 1*B* and in Tables 1 and 2, starting from the initial conditions described in Table S1 (included in the supplemental material) yielded a steady state that we call a *basal condition*. Table 4 shows that free polyamine concentrations and enzyme activities in this basal condition fit remarkably well to actual values estimated from experimental available data (58). Furthermore, simulations with different initial conditions for time-dependent variables and for different time increments gave the same basal condition steady state, indicating that our model is not sensitive to initial conditions and does not exhibit numerical artifacts.

To check the influence of the tuned parameters on the model behavior, we tested simulations with variations in their values covering 4 orders of magnitude. For this, in each new simulation, one (and only one) of the tuned parameter values was

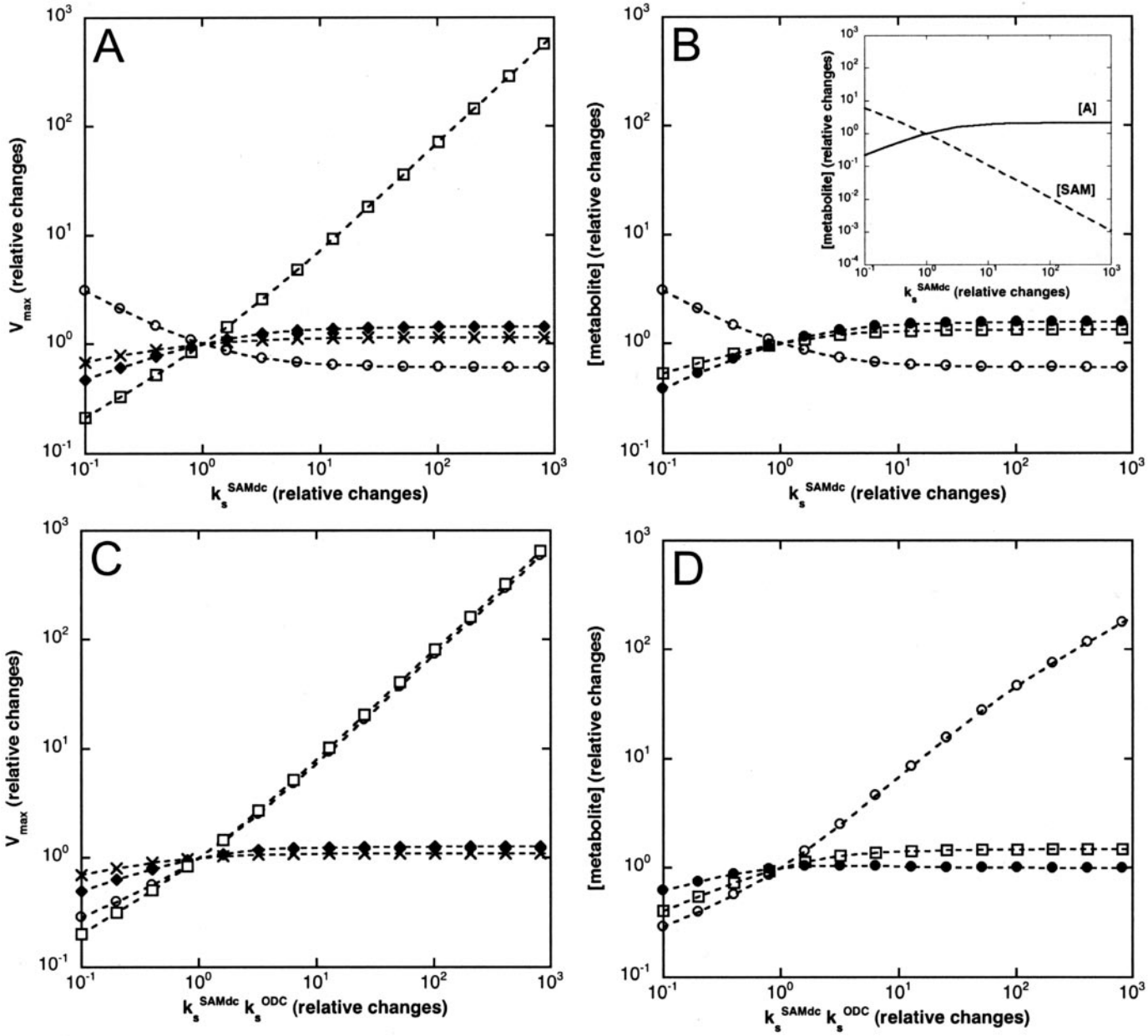

FIGURE 4. **Effects of changes in SAMdc k_S (*A* and *B*) and k_S for both SAMdc and ODC at the same time (*C* and *D*) on time-dependent activities (*A* and *C*) (ODC (*empty circles*), Antz (*crosses*), SSAT (*black diamonds*), and SAMdc (*empty squares*)) and on metabolite levels (*B* and *D*) (putrescine (*empty circles*), spermidine (*empty squares*), and spermine (*full circles*)), relative to the basal condition steady state.** *B* (*inset*), changes in the concentrations of SAM and decarboxylated SAM (*A*).

multiplied by 0.1 or 100. In all cases, steady state conditions were reached.

A way to test the capabilities of the model to respond to changes is to study the influence of the different parameters on the behavior of time-dependent variables (*i.e.* to carry out a sensitivity analysis) (61). Moreover, great changes in sensitivity coefficients can be taken as a probe of model failure, since a great change in a time-dependent variable caused by a little change in a parameter is not frequently found in this kind of mathematical model (62–64). The sensitivity analysis for all of the parameters and variables shows the robustness of our model, as detailed in the supplemental materials (under "Results from the Sensitivity Analysis of the Model"; see Table S2).

Model Predicts Compensatory Mechanisms to Keep Polyamine Homeostasis in Response to ODC Alterations by either Genetic or Pharmacological Intervention—Much experimental data has shown that changes in ODC expression have a prognostic value concerning cell transformation (65, 66). Polyamine depletion prevents cell proliferation, and ODC has been suggested as a therapeutic target in proliferative disorders, since it is a main factor responsible for the *de novo* synthesis of polyamines (31, 67, 68). In fact, knock-out ODC mice were not viable by failure in embryogenesis at the earliest stages (69, 70), showing that *de novo* synthesis must be essential in some cellular and embryonic processes. However, polyamine levels have proved to be very robust against alterations of ODC contents. ODC can be inactivated by its irreversible inhibitor DFMO. Many

studies using DFMO have shown effective depletion of putrescine and spermidine, whereas spermine content is often unaffected. DFMO has been described as a cytostatic rather than cytotoxic drug in cancer therapy (71). Moreover, its use in clinical chemotherapy has not shown as great results as initially expected (31). On the other hand, overexpressing ODC transgenic mice do not show increased levels of spermidine and spermine (72).

In our model, an increase of putrescine as a consequence of ODC expression modulation could be reached either by simulating an ODC overexpression or by simulating the effects of polyamines on antizyme translation (45) by changing their k_S values. Putrescine could also be increased by affecting enzymes related to back conversion of polyamines. However, in this case, the putrescine increase would be a consequence and not a cause of polyamine depletion, as we will see later. Fig. 2 (*A* and *B* for ODC and *C* and *D* for antizyme) shows the relative changes of the steady state values as compared with basal condition when k_S for each enzyme regulated by the Schimke equation is modified in a range that covers 5 orders of magnitude (0.1–1000-fold increases of its value in basal conditions, as mentioned under "Materials and Methods"). Antizyme decreased ODC levels, affecting neither the other enzymes nor higher polyamine (spermidine and spermine) levels. Acetyl-CoA and SAM levels remained unaffected (results not shown). ODC and antizyme increases only affected putrescine levels, as suggested by the sensitivity analysis for these enzymes (see Table S2). This is in agreement with experimental data on overexpressing ODC transgenic mice, where polyamine levels are unaltered while putrescine is highly increased (72, 73). In our model, only when putrescine appeared to be limiting (simulated by ODC down-regulation), spermine levels were slightly modified (Fig. 2, *B* and *D*), in agreement with DFMO treatment simulation results, as shown and discussed below.

To check the influence of ODC suppression on the behavior of the system, we simulated a treatment with DFMO. Fig. 3 shows the time responses to a DFMO treatment obtained with simulations of our model and compared with experimental data (58). Our simulations predict very well the real experimental responses, with a drastic decrease of putrescine that caused a slight increase of SAM (results not shown), followed by a decrease of spermidine and a slight increase of spermine. The same tendencies, but more attenuated, were also observed for 0.1-fold ODC activity down-regulation (Fig. 2). In fact, such results were already seen in simulations of the core system model (Table 3 and results not shown).

Summarizing the results of simulated ODC modulations, our model predicts very well the available experimental data, showing that dramatic changes in putrescine levels are not accompanied by similar changes in the levels of higher polyamines (spermidine and spermine), at least in the short term. This robustness of polyamine metabolism against alterations in the key enzyme ODC has been suggested to be due to compensating alterations in the rate of exogenous polyamine uptake, since antizyme behaves as an inhibitor of the transporter (74). In addition to this transport-dependent effect, our simulations suggest that a transport-independent component (the regulatory mechanism of the bi-cyclic pathway) also contributes to this robustness. This fact and the proven importance of ODC in cell transformation could suggest that putrescine could serve not only as a requested substrate for spermidine (and spermine) synthesis but also as a regulatory signal of cell proliferation. It has been shown that peaks of putrescine occur in different phases of the cell cycle (29, 75). Furthermore, putrescine stimulates tyrosine phosphorylation by tyrosine kinases and the expression of the nuclear oncogenes c-*fos* and c-*jun* (35).

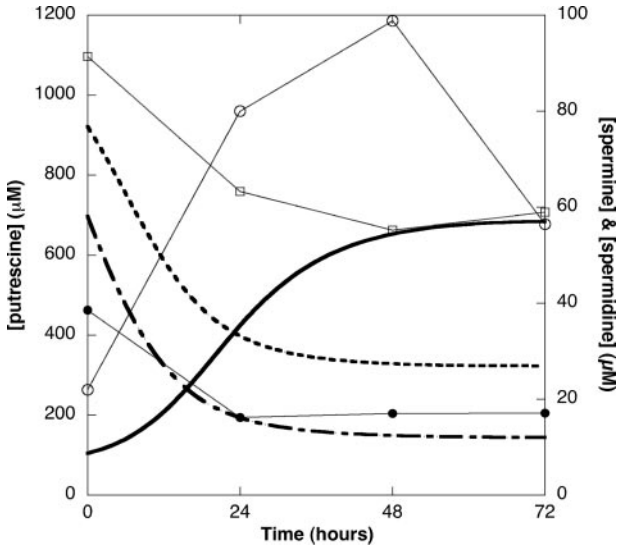

FIGURE 5. **MGBG effects on polyamine levels in both time-response simulations and data extracted from Ref. 58.** *In silico* experiments are shown as follows: putrescine (*continuous line*), spermidine (*dotted line*), and spermine (*segment and dotted line*). Experimental data are shown as follows: putrescine (*empty circles*), spermidine (*empty squares*), and spermine (*full circles*).

Model Predicts the Effects of SAMdc Modulation in Accordance with Experimental Data Obtained Using Transgenic Mice and Inhibitors—Synthesis of spermidine and spermine does not only require putrescine but also an aminopropyl donor, namely decarboxylated *S*-adenosylmethionine, the product of SAMdc activity. Therefore, it could be argued that SAMdc induction would cause an increase in the levels of higher polyamines. Under this hypothesis, great efforts have been devoted to obtaining SAMdc-overexpressing or knocked out transgenic mice. As it happens with ODC, SAMdc knock-outs are lethal at the earliest stages of embryonic development (76). SAMdc-overexpressing mice show modest inductions (5-fold increase) (49), with only small changes of higher polyamine levels. In a recently published work, >100-fold inductions have been obtained with little variation of polyamine content (77). Such works and others with SAMdc-overexpressing cells (78–80) show that putrescine decreases. However, a cross-breeding of ODC- and SAMdc-overexpressing transgenic mice shows that putrescine is not limiting in polyamine synthesis, and those mice still maintain a polyamine homeostasis. Heljasvaara *et al.* (49) suggest that, since polyamine accumulation is toxic, a homeostasis is not unexpected. Indeed, they proved that this homeostasis is reached by an increased rate of the bi-cycle, with a faster polyamine synthesis followed by an increase of acetylated polyamine efflux, although they could not find any direct evidence of increased SSAT activity (49).

Simulations of SAMdc and SAMdc/ODC overexpression (Fig. 4) predict a very remarkable buffering of the levels of

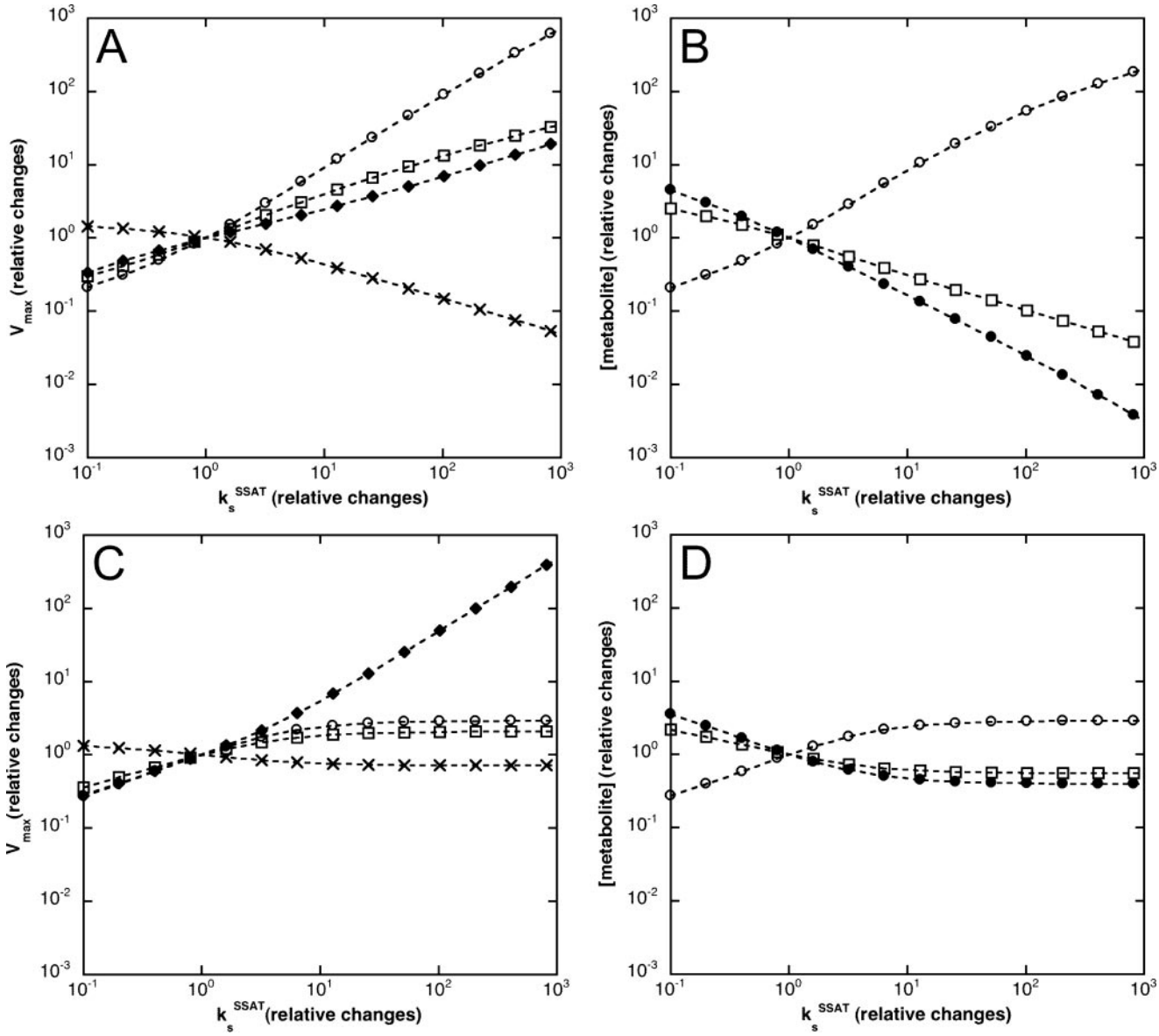

FIGURE 6. **Effects of changes in SSAT k_S for two values of the R parameter, that of basal conditions (*panels A* and *B*) and that corresponding to a 25% of the basal conditions value (*C* and *D*) on time-dependent activities (*A* and *C*) (ODC (*empty circles*), Antz (*cross*), SSAT (*full triangles*), and SAMdc (*empty squares*)) and on metabolite levels (*B* and *D*) (putrescine (*empty circles*), spermidine (*empty squares*), and spermine (*full circles*)) relative to the basal condition steady state.**

higher polyamines, in agreement with available experimental data (49, 77). However, we only observed such a tendency when we extended the core system model to consider the production of SAM from methionine. In our model depicted in Fig. 1*B*, simulations of SAMdc activity overexpression showed that SAM levels changed linearly with variations in the relative levels of SAMdc, maintaining well buffered levels of decarboxylated SAM to feed the polyamine metabolism bi-cycle (see *inset* in Fig. 4*B*). Based on these observations, we suggest that the branch of SAM production in the methyl cycle pathway could be relevant for polyamine homeostasis. However, there are no available experimental data to test this hypothesis currently.

The use of the competitive inhibitor MGBG is an alternative approach to analyze the effects of an inhibition of SAMdc activity. MGBG increases putrescine levels and diminishes higher polyamines (58, 71, 81). Actual experimental data on pharmacological inhibition with high doses of the reversible inhibitor MGBG are also remarkably well predicted with simulations of partial inhibition of SAMdc activity (Fig. 5).

Simulations of Changes of Acetyl-CoA Availability Predict the Responses to SSAT Induction Observed in Experimental Models—SSAT is described as the key enzyme for polyamine catabolism (43, 82). In SSAT-induced experimental models, a remarkable accumulation of putrescine and decreases of spermidine and spermine levels are observed (83–86). However, it should be stressed that steady state polyamine levels in experimental SSAT-overexpressing models can vary in a wide range, depending on the actual SSAT induction reached. This is true even for data published by the same group (51, 87).

In our model (Fig. 1*B*), acetyl-CoA availability is controlled by the *R* parameter (used to estimate the rate of recycling).

Simulations of SSAT level variations exhibited two different behaviors depending on the availability of acetyl-CoA for the degradation pathway. Fig. 6 (*A* and *B*) shows that polyamine depletion is allowed when the requirements of acetyl-CoA are satisfied. This occurs in our model when *R* is high (Fig. 7). However, when the *R* value is reduced to 25% of its value under basal conditions, a new physiological steady state slightly different from the previous one is achieved (78 μM putrescine, 91 μM spermidine, and 76 μM spermine). Under these new basal conditions, a SSAT overexpression causes only modest changes in the levels of polyamines (Fig. 6, *C* and *D*), as seems to be the case for most of the available experimental data with transgenic mice (51, 86, 88, 89). Acetyl-CoA levels do not change with increasing SSAT expression under basal conditions of recycling (Fig. 6*B*). In contrast, for *R* values reduced to 25% of the value under basal conditions, acetyl-CoA levels drop with increasing SSAT expression (Fig. 6*D*). This observation suggests that, in fact, acetyl-CoA availability determines the actual changes in polyamine induced by SSAT overexpression.

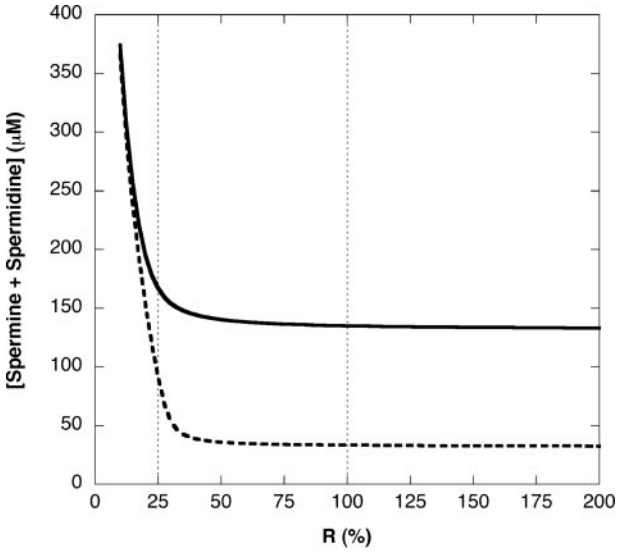

FIGURE 7. **Effects of acetyl-CoA recycling rate in the free polyamine levels once steady state is reached.** *Continuous line*, basal conditions; *dashed line*, 10-fold induced SSAT basal activity conditions. In this case, SSAT activity is considered a time-independent parameter. *Vertical dashed lines* define the *R* conditions used for the SSAT induction simulations described under "Results and Discussion."

Model Predicts the Effects of the Polyamine Analog DENSPM on Polyamine Metabolism Observed with Experimental Data—DENSPM is a polyamine analog described as one of the most potent inducers of SSAT (90). Furthermore, it also reduces ODC and SAMdc activities (58, 90). These joined effects lead to polyamine depletion (87, 91). To simulate the effects of DENSPM in our model, we assumed that this unmetabolizable analog causes its effect by a modulation of synthesis and degradation constants for those enzymes ruled by the Schimke equation. Experimental measurements of intracellular DENSPM after 24 h of incubation in culture cells were around 1000 μM, as calculated from data described by Korhonen *et al.* (58). Thus, we modified the Schimke equation for each enzyme by adding this concentration value to the polyamine pool (*i.e.* $(S + D)$ was changed by $(S + D + 1000)$, and simulation was restarted from basal conditions of the modified model. Fig. 8*B* shows that the time response of a DENSPM treatment on polyamine levels predicted by simulations of our model fits well to experimental data (58, 90, 92). It should be stressed that higher polyamine depletion predicted by DENSPM treatment is more drastic than those caused by a SSAT overexpression (compare Fig. 8*B* with Fig. 6) and a SAMdc inhibition (compare Fig. 8*B* with Fig. 5). Furthermore, in this case of DENSPM treatment, all three polyamines, including putrescine, were depleted. Fig. 8*A* shows that DENSPM treatment increased SSAT and decreased ODC and SAMdc activities, in agreement with the tendencies described by real experimental data (58).

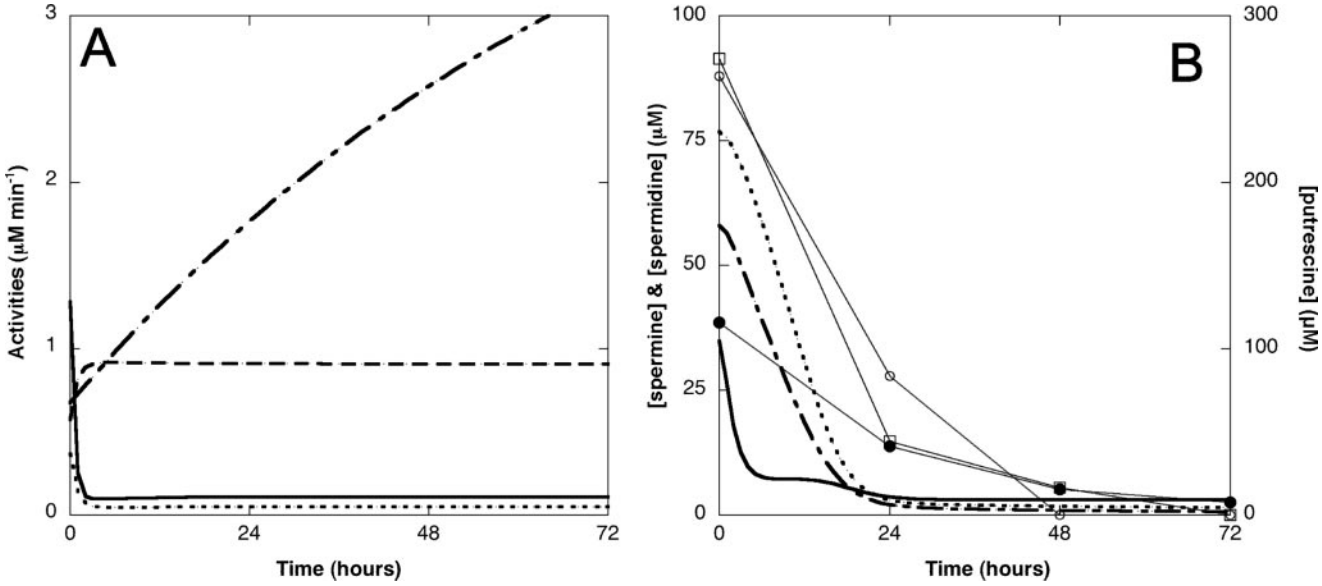

FIGURE 8. **DENSPM effects on short lived enzymes and polyamine levels.** *A*, predicted effects on enzymes, ODC (*continuous line*), Antz (*dashed line*), SAMdc (*dotted line*), and SSAT (*segment and dotted line*). *B*, effects on polyamines in both time-response simulations and data extracted from Ref. 58. *In silico* experiments are shown as follows: putrescine (*continuous line*), spermidine (*dotted line*), and spermine (*segment and dotted line*). Experimental data are shown as follows: putrescine (*empty circles*), spermidine (*empty squares*), and spermine (*full circles*).

Conclusion—Herein, we describe the first mathematical model proposed for mammalian polyamine metabolism. Modeling is a process of simplification of real biological phenomena that imposes severe limitations and restrictions. However, the essence of modeling is also to obtain the simplest model able to explain the majority of cases. In this context, a model as complex as reality is useless to acquire a comprehensive understanding of experimental evidence. The ultimate goal of this work is not just to mimic the biochemistry of polyamine metabolism but also to define the minimal study system that we should have to take into account, in both experimental and theoretical approaches, to understand how this complex pathway performs its biological function and responds to genetic and environmental perturbations. A minimal study system definition is possible based on the modular architecture of metabolism (93). The topology of the system (shown in Fig. 1) is relatively complex, with a central bi-cycle, two requested entrances, and two alternative exits. Furthermore, some of the enzymes involved in this metabolic pathway exhibit remarkable regulatory features, which have been taken into account to formulate the basic model. On the other hand, the unhomogeneous quality of the sparse and disperse experimental data concerning polyamine metabolism in mammals is another limitation. Despite all of these constraints, the described mathematical model fulfils the initial goals, contributing to increase our understanding of polyamine metabolism and to predict the adaptative response of this pathway to genetic and environmental perturbations. In addition, our iterative model refinement process has allowed us to suggest a minimal study system of polyamine metabolism in which SAM and acetyl-CoA availability appears as an additional factor to explain controversial results, such as the diversity of behaviors observed when SSAT is induced and polyamine homeostasis when SAMdc is induced. Obviously, this model does not try to mimic the reality in all of the situations, and the results have to be taken as a plausible explanation and integration of sparse data compiled through almost 30 years of polyamine research. In contrast with top-down metabolic flux control analysis methods (61, 94), our model represents a bottom-up approach to an understanding of complex metabolic networks, as is the case for other recently published models (8–10).

We have shown that our model of polyamine interconversion reflects some critical features observed in experimental approaches, such as ODC modulation, polyamine depletion by SSAT induction, and responses to polyamine analog exposure, among others. Results from our simulations include predictions on changes in antizyme contents (Figs. 4 and 6, *A* and *C*) not discussed in this work, which could be tested experimentally. The fact that polyamine analogs can produce such potent depletions of polyamine levels as those described in literature and predicted by our model can be due to synergic effects on more than one enzyme (87). This suggests that the combination of targets in order to alter polyamine levels could be a useful strategy to prevent polyamine-related diseases. However, from a technical point of view, the number of conditions needed to experimentally test the influence of n drugs is as high as 2^n. Furthermore, that huge number is correct considering only one replica, variable, and concentration to be tested. The use of mathematical models represents a helpful tool to restrict the actual number of real experiments to only those producing interesting results, according to the predictions based on model simulations. Moreover, a deeper analysis concerning parameter weights under different conditions could help us to identify conditions and targets to control polyamine levels.

As we would expect from systems and synthetic biology approaches, the predictions of this model could contribute to propose new hypotheses to be experimentally tested. In turn, the results of these experiments could contribute to the model refinement. In fact, this has already occurred, since some of the predictions of the core system model suggested that we had to introduce some changes to improve it, as verified with our proposed model. In this paper, we have proposed that alternative behaviors of SSAT overexpression can depend on acetyl-CoA availability, in agreement with experimental evidence (95). We have also suggested an explanation for the observed compatibility of ODC and SAMdc induction with polyamine homeostasis.

Such *in silico* results open new hypotheses to be tested by experimental work and can suggest predictions for conditions where viable transgenic mice have not yet been obtained. According to this, we suggest that SAM levels and acetyl-CoA availability should be taken into account in future experimental work to get a more complete view of this metabolism, as has already been the case in a study of the effects of activated polyamine catabolism in an *in vivo* model of prostate cancer (95). As more quantitative information about polyamine metabolism becomes available, it can be incorporated into the model, and further hypotheses can be tested. Of course, the model presented here is incomplete for many reasons, including those simplifications assumed *a priori* and mentioned in the description of the model. However, the modularity of complex, hierarchical biological systems allows relatively simple extensions of a metabolic model by the aggregation of additional modules, such as the one suggested in relation to the role of *S*-adenosylmethionine. Additional features, such as the expected relevant roles of polyamine uptake and detailed gene expression regulatory mechanisms would demand future modifications of the present model.

Acknowledgments—We thank Dr. A. Pegg for useful suggestions during manuscript preparation, Dr. C. Cotta for help during model construction, and M. Cánovas and V. Boucard-Mathey for language corrections. Valuable information input was also received from other member groups of European Cooperation in the field of Scientific and Technical Research Action 922 (supported by the European Science Foundation).

REFERENCES

1. Hartwell, L. H., Hopfield, J. J., Leibler, S., and Murray, A. W. (1999) *Nature* **402,** C47–C52
2. Alberghina, L., Chiaradonna, F., and Vanoni, M. (2004) *Chembiochem* **5,** 1322–1333
3. Kitano, H. (2001) *Foundations of Systems Biology*, The MIT press, London, UK
4. Kitano, H. (2002) *Science* **295,** 1662–1664
5. Benner, S. A., and Sismour, A. M. (2005) *Nat. Rev. Genet.* **6,** 533–543
6. Kitano, H. (2002) *Nature* **420,** 206–210

7. Weston, A. D., and Hood, L. (2004) *J. Proteome Res.* **3,** 179–196
8. Reed, M. C., Nijhout, H. F., Sparks, R., and Ulrich, C. M. (2004) *J. Theor. Biol.* **226,** 33–43
9. Nijhout, H. F., Reed, M. C., Budu, P., and Ulrich, C. M. (2004) *J. Biol. Chem.* **279,** 55008–55016
10. Yang, C. R., Shapiro, B. E., Hung, S. P., Mjolsness, E. D., and Hatfield, G. W. (2005) *J. Biol. Chem.* **280,** 11224–11232
11. Tabor, C. W., and Tabor, H. (1984) *Annu. Rev. Biochem.* **53,** 749–790
12. Heby, O., and Persson, L. (1990) *Trends Biochem. Sci.* **15,** 153–158
13. Urdiales, J. L., Medina, M. A., and Sanchez-Jimenez, F. (2001) *Eur. J. Gastroenterol. Hepatol.* **13,** 1015–1019
14. Medina, M. A., Urdiales, J. L., Rodriguez-Caso, C., Ramirez, F. J., and Sanchez-Jimenez, F. (2003) *Crit. Rev. Biochem. Mol. Biol.* **38,** 23–59
15. Medina, M. A., Correa-Fiz, F., Rodriguez-Caso, C., and Sanchez-Jimenez, F. (2005) *J. Cell Mol. Med.* **9,** 854–864
16. Cohen, S. S. (1998) *A Guide of Polyamines*, Oxford University Press, New York
17. Ruiz-Chica, J., Medina, M. A., Sanchez-Jimenez, F., and Ramirez, F. J. (2001) *Biophys. J.* **80,** 443–454
18. Brandes, L. J., Queen, G. M., and LaBella, F. S. (1998) *J. Cell. Biochem.* **69,** 233–243
19. Lesort, M., Tucholski, J., Miller, M. L., and Johnson, G. V. (2000) *Prog. Neurobiol.* **61,** 439–463
20. Esposito, C., and Caputo, I. (2005) *FEBS J.* **272,** 615–631
21. Seiler, N. (2005) *Pharmacol. Ther.* **107,** 99–119
22. Wallace, H. M., Fraser, A. V., and Hughes, A. (2003) *Biochem. J.* **376,** 1–14
23. Watanabe, S., Kusama-Eguchi, K., Kobayashi, H., and Igarashi, K. (1991) *J. Biol. Chem.* **266,** 20803–20809
24. Igarashi, K., and Kashiwagi, K. (2000) *Biochem. Biophys. Res. Commun.* **271,** 559–564
25. Wang, Y., Xiao, L., Thiagalingam, A., Nelkin, B. D., and Casero, R. A., Jr. (1998) *J. Biol. Chem.* **273,** 34623–34630
26. Wang, Y., Devereux, W., Woster, P. M., Stewart, T. M., Hacker, A., and Casero, R. A., Jr. (2001) *Cancer Res.* **61,** 5370–5373
27. Davis, R. H. (1990) *J. Cell. Biochem.* **44,** 199–205
28. Coffino, P. (2000) *Proc. Natl. Acad. Sci. U. S. A.* **97,** 4421–4423
29. Thomas, T., and Thomas, T. J. (2001) *Cell Mol. Life Sci.* **58,** 244–258
30. Pietila, M., Pirinen, E., Keskitalo, S., Juutinen, S., Pasonen-Seppanen, S., Keinanen, T., Alhonen, L., and Janne, J. (2005) *J. Invest. Dermatol.* **124,** 596–601
31. Gerner, E. W., and Meyskens, F. L., Jr. (2004) *Nat. Rev. Cancer* **4,** 781–792
32. Coffino, P., and Poznanski, A. (1991) *J. Cell. Biochem.* **45,** 54–58
33. Nilsson, J. A., Keller, U. B., Baudino, T. A., Yang, C., Norton, S., Old, J. A., Nilsson, L. M., Neale, G., Kramer, D. L., Porter, C. W., and Cleveland, J. L. (2005) *Cancer Cell* **7,** 433–444
34. Kramer, D. L., Vujcic, S., Diegelman, P., Alderfer, J., Miller, J. T., Black, J. D., Bergeron, R. J., and Porter, C. W. (1999) *Cancer Res.* **59,** 1278–1286
35. Bachrach, U., Wang, Y. C., and Tabib, A. (2001) *News Physiol. Sci.* **16,** 106–109
36. Kutuzov, M. A., Andreeva, A. V., and Voyno-Yasenetskaya, T. A. (2005) *J. Biol. Chem.* **280,** 25388–25395
37. Hu, X., Washington, S., Verderame, M. F., and Manni, A. (2005) *Cancer Res.* **65,** 11026–11033
38. Pegg, A. E., Feith, D. J., Fong, L. Y., Coleman, C. S., O'Brien, T. G., and Shantz, L. M. (2003) *Biochem. Soc. Trans.* **31,** 356–360
39. Pegg, A. E. (2006) *J. Biol. Chem.* **281,** 14529–14532
40. Huang, Y., Pledgie, A., Casero, R. A., Jr., and Davidson, N. E. (2005) *Anticancer Drugs* **16,** 229–241
41. Childs, A. C., Mehta, D. J., and Gerner, E. W. (2003) *Cell Mol. Life Sci.* **60,** 1394–1406
42. Wallace, H. M., and Mackarel, A. J. (1998) *Biochem. Soc. Trans.* **26,** 571–575
43. Seiler, N. (2004) *Amino Acids* **26,** 217–233
44. Seiler, N., Delcros, J. G., and Moulinoux, J. P. (1996) *Int. J. Biochem. Cell Biol.* **28,** 843–861
45. Ivanov, I. P., Matsufuji, S., Murakami, Y., Gesteland, R. F., and Atkins, J. F. (2000) *EMBO J.* **19,** 1907–1917
46. Murakami, Y., Matsufuji, S., Hayashi, S., Tanahashi, N., and Tanaka, K. (2000) *Biochem. Biophys. Res. Commun.* **267,** 1–6
47. Raina, A., Hyvonen, T., Eloranta, T., Voutilainen, M., Samejima, K., and Yamanoha, B. (1984) *Biochem. J.* **219,** 991–1000
48. Pajula, R. L. (1983) *Biochem. J.* **215,** 669–676
49. Heljasvaara, R., Veress, I., Halmekyto, M., Alhonen, L., Janne, J., Laajala, P., and Pajunen, A. (1997) *Biochem. J.* **323,** 457–462
50. Vujcic, S., Liang, P., Diegelman, P., Kramer, D. L., and Porter, C. W. (2003) *Biochem. J.* **370,** 19–28
51. Alhonen, L., Karppinen, A., Uusi-Oukari, M., Vujcic, S., Korhonen, V. P., Halmekyto, M., Kramer, D. L., Hines, R., Janne, J., and Porter, C. W. (1998) *J. Biol. Chem.* **273,** 1964–1969
52. Shappell, N. W., Fogel-Petrovic, M. F., and Porter, C. W. (1993) *FEBS Lett.* **321,** 179–183
53. Fogel-Petrovic, M., Shappell, N. W., Bergeron, R. J., and Porter, C. W. (1993) *J. Biol. Chem.* **268,** 19118–19125
54. Shantz, L. M., Holm, I., Janne, O. A., and Pegg, A. E. (1992) *Biochem. J.* **288,** 511–518
55. Bogle, R. G., Mann, G. E., Pearson, J. D., and Morgan, D. M. L. (1994) *Am. J. Physiol.* **284,** C776–C783
56. Pegg, A. E., McGovern, K. A., and Wiest, L. (1987) *Biochem. J.* **241,** 305–307
57. Seppanen, P., Fagerstrom, R., Alhonen-Hongisto, L., Elo, H., Lumme, P., and Janne, J. (1984) *Biochem. J.* **221,** 483–488
58. Korhonen, V. P., Niiranen, K., Halmekyto, M., Pietila, M., Diegelman, P., Parkkinen, J. J., Eloranta, T., Porter, C. W., Alhonen, L., and Janne, J. (2001) *Mol. Pharmacol.* **59,** 231–238
59. Berntsson, P. S., Alm, K., and Oredsson, S. M. (1999) *Biochem. Biophys. Res. Commun.* **263,** 13–16
60. Parry, L., Balana Fouce, R., and Pegg, A. E. (1995) *Biochem. J.* **305,** 451–458
61. Fell, D. (1997) in *Understanding the Control of Metabolism* (Snell, K., ed) Portland Press, London
62. Savageau, M. A. (1971) *Nature* **229,** 542–544
63. Savageau, M. A., Kotre, A. M., and Sakamoto, N. (1972) *Biochem. Biophys. Res. Commun.* **48,** 41–47
64. Morohashi, M., Winn, A. E., Borisuk, M. T., Bolouri, H., Doyle, J., and Kitano, H. (2002) *J. Theor. Biol.* **216,** 19–30
65. Auvinen, M., Laine, A., Paasinen-Sohns, A., Kangas, A., Kangas, L., Saksela, O., Andersson, L. C., and Holtta, E. (1997) *Cancer Res.* **57,** 3016–3025
66. Moshier, J. A., Dosescu, J., Skunca, M., and Luk, G. D. (1993) *Cancer Res.* **53,** 2618–2622
67. Pegg, A. E. (1988) *Cancer Res.* **48,** 759–774
68. Thomas, T., and Thomas, T. J. (2003) *J. Cell Mol. Med.* **7,** 113–126
69. Pendeville, H., Carpino, N., Marine, J. C., Takahashi, Y., Muller, M., Martial, J. A., and Cleveland, J. L. (2001) *Mol. Cell. Biol.* **21,** 6549–6558
70. Janne, J., Alhonen, L., Pietila, M., and Keinanen, T. A. (2004) *Eur. J. Biochem.* **271,** 877–894
71. Wallace, H. M., and Fraser, A. V. (2004) *Amino Acids* **26,** 353–365
72. Halmekyto, M., Alhonen, L., Alakuijala, L., and Janne, J. (1993) *Biochem. J.* **291,** 505–508
73. Halmekyto, M., Alhonen, L., Wahlfors, J., Sinervirta, R., Eloranta, T., and Janne, J. (1991) *Biochem. J.* **278,** 895–898
74. Mitchell, J. L., Simkus, C. L., Thane, T. K., Tokarz, P., Bonar, M. M., Frydman, B., Valasinas, A. L., Reddy, V. K., and Marton, L. J. (2004) *Biochem. J.* **384,** 271–279
75. Bettuzzi, S., Davalli, P., Astancolle, S., Pinna, C., Roncaglia, R., Boraldi, F., Tiozzo, R., Sharrard, M., and Corti, A. (1999) *FEBS Lett.* **446,** 18–22
76. Nishimura, K., Nakatsu, F., Kashiwagi, K., Ohno, H., Saito, T., and Igarashi, K. (2002) *Genes Cells* **7,** 41–47
77. Nisenberg, O., Pegg, A. E., Welsh, P. A., Keefer, K., and Shantz, L. M. (2006) *Biochem. J.* **393,** 295–302
78. Kramer, D., Mett, H., Evans, A., Regenass, U., Diegelman, P., and Porter, C. W. (1995) *J. Biol. Chem.* **270,** 2124–2132
79. Suzuki, T., Sadakata, Y., Kashiwagi, K., Hoshino, K., Kakinuma, Y., Shirahata, A., and Igarashi, K. (1993) *Eur. J. Biochem.* **215,** 247–253
80. Manni, A., Badger, B., Grove, R., Kunselman, S., and Demers, L. (1995) *Cancer Lett.* **95,** 23–28
81. Ferioli, M. E., Bottone, M. G., Soldani, C., and Pellicciari, C. (2004) *Cell*

Mol. Life Sci. **61,** 2767–2773
82. Casero, R. A., Jr., and Pegg, A. E. (1993) *FASEB J.* **7,** 653–661
83. Fogel-Petrovic, M., Vujcic, S., Miller, J., and Porter, C. W. (1996) *FEBS Lett.* **391,** 89–94
84. Fogel-Petrovic, M., Vujcic, S., Brown, P. J., Haddox, M. K., and Porter, C. W. (1996) *Biochemistry* **35,** 14436–14444
85. Pietila, M., Alhonen, L., Halmekyto, M., Kanter, P., Janne, J., and Porter, C. W. (1997) *J. Biol. Chem.* **272,** 18746–18751
86. Suppola, S., Heikkinen, S., Parkkinen, J. J., Uusi-Oukari, M., Korhonen, V. P., Keinanen, T., Alhonen, L., and Janne, J. (2001) *Biochem. J.* **358,** 343–348
87. Alhonen, L., Pietila, M., Halmekyto, M., Kramer, D. L., Janne, J., and Porter, C. W. (1999) *Mol. Pharmacol.* **55,** 693–698
88. Coleman, C. S., Pegg, A. E., Megosh, L. C., Guo, Y., Sawicki, J. A., and O'Brien, T. G. (2002) *Carcinogenesis* **23,** 359–364
89. Tucker, J. M., Murphy, J. T., Kisiel, N., Diegelman, P., Barbour, K. W., Davis, C., Medda, M., Alhonen, L., Janne, J., Kramer, D. L., Porter, C. W., and Berger, F. G. (2005) *Cancer Res.* **65,** 5390–5398
90. Pegg, A. E., Wechter, R., Pakala, R., and Bergeron, R. J. (1989) *J. Biol. Chem.* **264,** 11744–11749
91. Schipper, R. G., Deli, G., Deloyer, P., Lange, W. P., Schalken, J. A., and Verhofstad, A. A. (2000) *Prostate* **44,** 313–321
92. Hector, S., Porter, C. W., Kramer, D. L., Clark, K., Prey, J., Kisiel, N., Diegelman, P., Chen, Y., and Pendyala, L. (2004) *Mol. Cancer Ther.* **3,** 813–822
93. Ravasz, E., Somera, A. L., Mongru, D. A., Oltvai, Z. N., and Barabasi, A. L. (2002) *Science* **297,** 1551–1555
94. Edwards, J. S., Ibarra, R. U., and Palsson, B. O. (2001) *Nat. Biotechnol.* **19,** 125–130
95. Kee, K., Foster, B. A., Merali, S., Kramer, D. L., Hensen, M. L., Diegelman, P., Kisiel, N., Vujcic, S., Mazurchuk, R. V., and Porter, C. W. (2004) *J. Biol. Chem.* **279,** 40076–40083
96. Pegg, A. E., and Poso, H. (1983) *Methods Enzymol.* **94,** 234–239
97. Ragione, F. D., and Pegg, A. E. (1982) *Biochemistry* **21,** 6152–6158
98. Martinov, M. V., Vitvitsky, V. M., Mosharov, E. V., Banerjee, R., and Ataullakhanov, F. I. (2000) *J. Theor. Biol.* **204,** 521–532